

Low-Temperature Performance of Nanoscale Perpendicular Magnetic Tunnel Junctions With Double MgO-Interface Free Layer

Kaihua Cao^{1,2,3}, Huisong Li¹, Wenlong Cai¹, Jiaqi Wei^{1,2,3}, Lezhi Wang^{1,2,3}, Yanpeng Hu³, Qifeng Jiang³, Hushan Cui^{2,3}, Chao Zhao^{2,3}, and Weisheng Zhao^{1,2,4}

¹Fert Beijing Institute, BDBC, Beihang University, Beijing 100191, China

²School of Electronic and Information Engineering, Beihang University, Beijing 100191, China

³Institute of Microelectronics of Chinese Academy of Sciences, Beijing 100029, China

⁴Beihang-Geortek Joint Microelectronics Institute, Qingdao Research Institute, Beihang University, Qingdao 266000, China

The temperature dependence of magnetoresistance and switching characterization based on spin transfer torque (STT) effect of perpendicular magnetic tunnel junctions (p-MTJs) with MgO/CoFeB/W/CoFeB/MgO double-interface free layer was studied. The tunneling magnetoresistance (TMR) ratio increases from 95% to 176% for both 84 and 64 nm-diameter p-MTJs, upon decreasing the temperature from 400 to 20 K. This change of TMR is dominated by a steady increase in the resistance of antiparallel state while the parallel state conductance remains almost constant. Switching behavior at various temperatures is investigated for pulse voltage-dependent STT measurements; resistance versus voltage loops for both the switching directions become more symmetric with decreasing temperature. Furthermore, low-temperature measurements of magnetic properties suggest that the effect of stray field for STT becomes weaker as the temperature decreases, which suggests the p-MTJs design for cryogenic memories.

Index Terms—Perpendicular magnetic tunnel junction (p-MTJ), spin transfer torque (STT), spintronics, temperature dependence.

I. INTRODUCTION

PERPENDICULAR magnetic tunnel junction (p-MTJ) combined with the spin transfer torque (STT) mechanism is regarded as a promising non-volatile memory device owing to its high speed, energy efficiency, scalability, and infinite endurance [1]–[4]. Parallel to efforts to reduce power consumption in memory storage devices, there is a novel approach toward superconducting computing operating at a temperature of 4 K [5], [6]. In order to satisfy the needs of superconductor-based processors, cryogenic memories that operate in proximity with the superconducting circuitry are required.

CoFeB-MgO p-MTJ devices, where perpendicular magnetic anisotropy originates from interfacial anisotropy both at CoFeB/MgO and CoFeB/heavy metal interfaces [7]–[9], are potential candidates to meet major requirements for integrating the p-MTJs with computing circuits [10]. In addition, p-MTJs with a double MgO/CoFeB interface free layer, i.e., MgO/CoFeB/Ta/CoFeB/MgO, have been proved to possess a considerable tunneling magnetoresistance (TMR) ratio, thermal stability, and STT switching energy comparable to that of p-MTJ with a single interface [11]–[14]. Furthermore, the TMR has been shown to exhibit a strong dependence on temperature in previous theoretical and experimental works [15]–[22]. On the other hand, only a few experi-

mental studies deal with the temperature dependence of the performance of the nanoscale p-MTJs with double MgO-interface free layer structure. Therefore, quantifying the temperature dependence of both TMR ratio and STT effects is an important requirement for the design of emerging memory and logic devices, and cryogenic memories.

In this paper, we report the experimental results of the temperature dependence of the TMR and STT switching in the nanoscale p-MTJs with MgO/CoFeB/W/CoFeB/MgO double-interface free structure. The spin-dependent resistance and STT switching voltage of p-MTJs having 64 or 84 nm diameter were investigated at various temperatures from 400 to 20 K. We also studied the effect of the magnetic properties on STT switching at low temperature.

II. EXPERIMENTAL PROCEDURES

The p-MTJ stacks we studied here were composed of, from the substrate side, Ta(5)/Ru(30)/Ta(0.7)/Pt(1.5)/6x[Co(0.5)/Pt(0.2)]/Co(0.6)/Ru(0.8)/Co(0.6)/3x[Pt(0.2)/Co(0.5)]/W(0.25)/CoFeB(1.0)/MgO(0.8)/CoFeB(1.3)/W(0.25)/CoFeB(0.5)/MgO(0.75)/Pt(0.4)/Ta(0.3)/Ru(8) [Fig. 1(a), nominal thickness in nm]. These layers were deposited on thermally oxidized Si substrate by a Singulus magnetron-sputtering machine, where the MgO layers were deposited by RF magnetron sputtering whereas the other layers were deposited by dc magnetron sputtering. The deposited stacks were post-annealed in vacuum at 400 °C for 1 h without any external magnetic field. Then, the junctions were fabricated using electron beam lithography and Ar ion milling to pattern the free and reference layers separately. During free layer milling, we monitored the secondary-ion mass spectra and stopped

Manuscript received July 12, 2018; revised September 26, 2018; accepted October 14, 2018. Date of publication November 12, 2018; date of current version February 15, 2019. Corresponding authors: C. Zhao and W. Zhao (e-mail: zhaochao@ime.ac.cn; weisheng.zhao@buaa.edu.cn).

Color versions of one or more of the figures in this paper are available online at <http://ieeexplore.ieee.org>.

Digital Object Identifier 10.1109/TMAG.2018.2877446

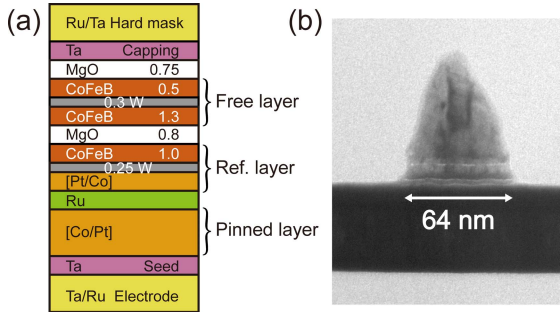


Fig. 1. (a) Schematic of the p-MTJ stack structure with MgO/CoFeB/W/CoFeB/MgO free layer. (b) Representative cross-sectional TEM image of a p-MTJ nanopillar ($D \sim 64$ nm).

the milling operation on the detection of signal through the 0.8 nm-thick MgO barrier.

Transport properties of the p-MTJs were measured using conventional two-probe techniques, and variable-temperature characterizations were performed in a helium cryostat (Lake shore CRX-VF cryogenic probe station with a temperature range of 20–450 K). Pulsed measurements were conducted using a Keithley 4200-SCS semiconductor characterization system. A positive bias corresponds to the arrangement of current flowing from the top to bottom electrodes.

III. RESULTS AND DISCUSSION

In order to reduce the stray field acting on free layer from reference layer, a stepped structure was employed where the reference and pinned layers were kept wider than the free layer [23]. This stepped structure requires an etching process that stops at the tunnel barrier. Fig. 1(b) shows the corresponding cross-sectional high-resolution transmission electron microscopy (TEM) image for a nanopillar, which reveals that the diameter (D) of the free layer is approximately 64 nm.

A. Temperature Dependence of TMR Ratio

The magnetotransport properties of the p-MTJs were measured under constant -50 mV bias voltage across the p-MTJs at various temperatures between 20 and 400 K. Fig. 2(a) and (d) shows the minor loops of magnetoresistance versus perpendicular external magnetic field (MR-H) at 300 K for the nanoscale p-MTJ devices with diameters of about 84 and 64 nm, respectively. The diameter of each p-MTJs was electrically estimated from its parallel state (R_P) and resistance-area product (RA; approximately $10 \Omega \cdot \mu\text{m}^2$) and was confirmed by TEM images. Fig. 2(b) and (e) presents the temperature dependencies of resistance in parallel and antiparallel (R_{AP}) states. For both the p-MTJs, from 400 to 20 K, the values for R_{AP} increased by about 40%, but the values of R_P did not show any significant change.

By computing the TMR ratio by $[(R_{AP} - R_P)/R_P]$, we obtained the temperature dependence of TMR ratio for 84 and 64 nm p-MTJs for temperatures from 400 to 20 K. Fig. 2(c) and (f) shows that the TMR ratio is around 96% and 95% at 400 K and increased to 176% at 20 K. This results in $\text{TMR}(20 \text{ K})/\text{TMR}(400 \text{ K}) = 1.85$; this change in TMR ratio

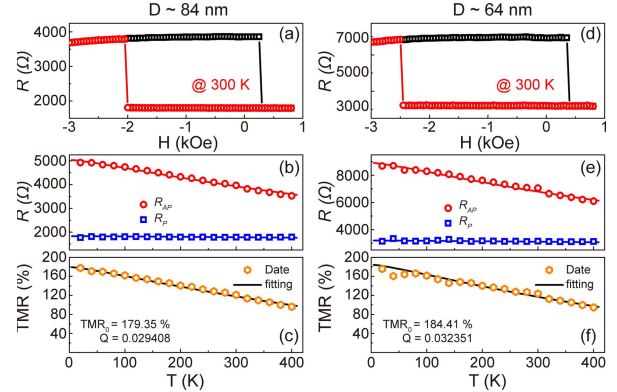


Fig. 2. (a) and (d) Magnetoresistance versus external magnetic field (MR-H) loops, measured at room temperature (300 K) and -50 mV dc bias voltage, of the nanoscale p-MTJ devices with diameter 84 and 64 nm, respectively. Temperature dependencies of (b) and (e) resistance of the parallel state (open squares) and the antiparallel state (open circles) and (c) and (f) TMR ratio for 84 and 64 nm diameter p-MTJ devices, respectively.

is dominated by a steady increase in R_{AP} with decreasing temperature.

Elastic and inelastic tunneling phenomena usually explain the temperature dependence of the resistances of MTJ [1], [15]. In this simple model, the temperature dependence of TMR ratio at low bias voltage can be deduced [24] from the following equation:

$$\text{TMR}(T) = (\text{TMR}_0 + 1) / \left(1 + 2Q \cdot \beta_{AP} \cdot \ln \left(\frac{k_B T}{E_C} \right) \right) - 1 \quad (1)$$

where TMR_0 is the TMR ratio at zero temperature, $T = 0$ K, and Q describes the probability of a magnon involved in the tunneling process that will be used as a fitting parameter. $\beta_{AP} = Sk_B T/E_m$, where S is the spin parameter, k_B is Boltzmann's constant, E_m is related to the Curie temperature $E_m = 3k_B T/(S + 1)$ of the ferromagnetic electrodes, and E_c is the magnon energy cutoff energy [25]. Fig. 2(c) and (f) displays the temperature dependence of TMR ratio for p-MTJ devices. Fitting the experimental data using (1) gives $\text{TMR}_0 = 179\%$ and 184% and $Q = 0.0294$ and 0.0324 for 84 and 64 nm p-MTJs, respectively. These values are of the same order as those previously reported for in-plane MTJ [1].

B. Temperature Dependence of Switching Voltage by STT

To study the temperature dependence of STT switching characteristics, we used the method of extracting the magnetic energy barrier (E_b) through pulse voltage-dependent STT measurements, which expresses the switching voltage (V_C) as a function of temperature [10] as shown in the following:

$$V_C^{P(AP)} = V_{C0}^{P(AP)} \left[1 - \frac{k_B T}{E_b^{P(AP)}} \ln \left(\frac{t_p}{\tau_0} \right) \right] \quad (2)$$

where $V_C^{P(AP)}$, $V_{C0}^{P(AP)}$, and $E_b^{P(AP)}$ are the parameters of the initial magnetization configuration before the magnetization reversal occurs, and superscripts P and AP represent parallel and antiparallel, respectively. V_{C0} is the intrinsic critical

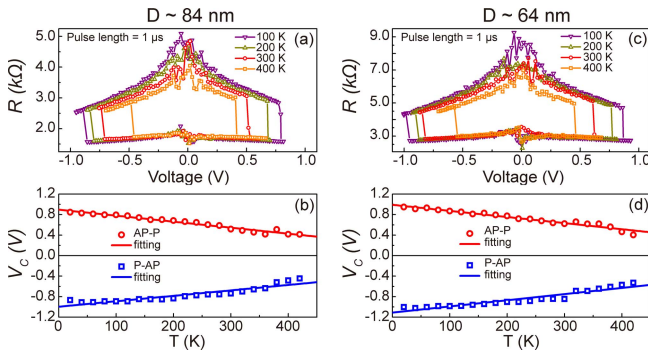


Fig. 3. (a) and (c) Resistance versus applied voltage pulse (R - V) curves, measured at various temperatures and $1\ \mu\text{s}$ pulselength, of the nanoscale p-MTJ devices with 84 and 64 nm diameter, respectively. Temperature dependence of (b) and (d) switching voltage of the P to AP (open squares) and the AP to P (open circles) for 84 and 64 nm-diameter p-MTJ devices, respectively, along with the theoretical fits.

switching voltage, t_p is the duration ($1\ \mu\text{s}$) of the applied voltage pulse, and τ_0 is the inverse of attempt frequency (assumed to be $1\ \text{ns}$).

Fig. 3(a) and (c) presents the resistance versus applied voltage pulse (R - V) house curves measured at various temperatures and $1\ \mu\text{s}$ pulselength of the nanoscale p-MTJ devices with 84 and 64 nm diameter, respectively. As shown in Fig. 3(a) and (c), the resistance values in parallel state of both p-MTJs did not have a significant change until the temperature decreased from 400 to 100 K and remained almost the same for various voltages. R_{AP} and V_C both increased when the temperature decreased in the case of both the p-MTJs. In addition, it is obvious that R_{AP} decreases with reading bias voltage [26], [27].

The $V_C^{P(AP)}$ as a function of temperature for both p-MTJs is shown in Fig. 3(b) and (d). As shown in Fig. 3(b) and (d), the $V_C^{P(AP)}$ of 84 and 64 nm p-MTJs are $-0.52 \pm 0.51\ \text{V}$ and $-0.57 \pm 0.46\ \text{V}$ at $400\ \text{K}$ and increase to $-0.87 \pm 0.85\ \text{V}$ and $-1.0 \pm 0.95\ \text{V}$ at $20\ \text{K}$, respectively. The P-AP and AP-P switching both increase when the temperature decreases for both the p-MTJs. On fitting the experimental data with (2), we got $V_{C0}^{P(AP)} = -0.99 \pm 0.89\ \text{V}$ and $-1.11 \pm 0.99\ \text{V}$ for 84 and 64 nm p-MTJs, respectively. The values of $V_{C0}^{P(AP)}$ of 64 nm p-MTJ are larger than those of 84 nm p-MTJ, indicating that the anisotropy field increases for decreasing junction sizes [28].

C. Temperature Dependence of Magnetic Properties

As mentioned above, V_{C0}^P is much larger than V_{C0}^{AP} for both p-MTJs. Combined with the observed asymmetry in MR- H loops, this suggests that there is a stray field assisting AP-P but preventing P-AP switching. The stray field arises from the imbalance of synthetic antiferromagnetic structure, which was caused by the over-etch and magnetic damage to the reference layer [29], [30].

In particular, the STT switching curves for both the states become more symmetric as temperature is decreased to $20\ \text{K}$, indicating that V_C^P/V_C^{AP} spin-torque efficiencies are becoming balanced. Asymmetric curves are observed at increased

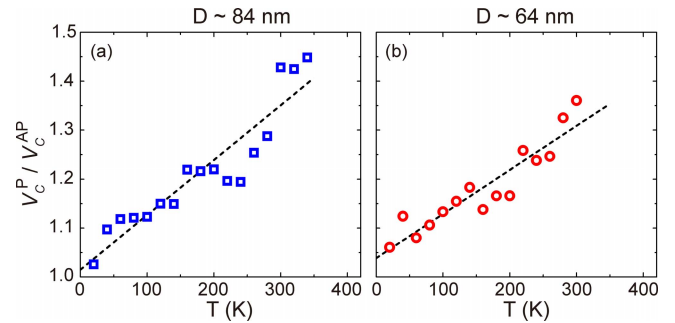


Fig. 4. STT switching asymmetry versus temperature measured by extracting V_C^P/V_C^{AP} for (a) 84 and (b) 64 nm-diameter p-MTJs, respectively.

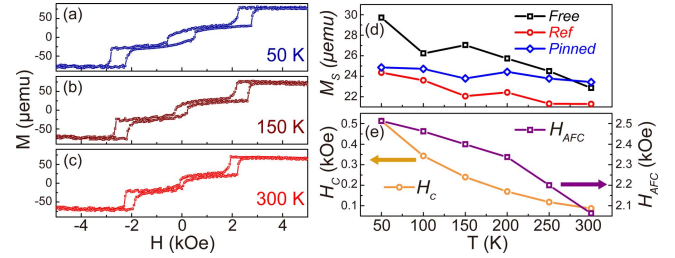


Fig. 5. Magnetic moment versus external magnetic field (M - H) loops measured at (a) 50, (b) 150, and (c) 300 K of the p-MTJ stack film. Temperature dependence of (d) saturation magnetization of the free layer (black open squares), reference layer (red open circles), and pinned layer (blue open diamond), and (e) coercive field (orange open circles) and antiferromagnetic coupling field (purple open squares) for a p-MTJ film.

temperatures, as shown in Fig. 4(a) and (b). In order to evaluate the temperature dependence of STT switching voltage, a negative 500 Oe external magnetic field must be provided when the temperature increases to 380 and 320 K for 84 and 64 nm p-MTJs, respectively, as shown in Fig. 3.

The temperature dependence of magnetic properties was independently investigated on a $3\ \text{mm} \times 3\ \text{mm}$ sample with a full stack film, which corresponds to the stacks used to fabricate the p-MTJs. Fig. 5(a)-(c) shows measurements of the magnetic moment (M) as a function of out-of-plane magnetic field (H_z) for temperatures ranging from 50 to 300 K, using a physical properties measurement system-vibrating sample magnetometer. These measurements confirmed that the top and bottom CoFeB free layers present strong ferromagnetic coupling, whereas the reference and pinned layers exhibit strong antiferromagnetic coupling.

Fig. 5(d) demonstrates a weaker dependence of the saturation magnetization (M_s) on temperature for free, reference, and pinned layers, and shows good agreement with the previous reports [31]. At the same time, a strong temperature dependence of the coercivity, as shown in Fig. 5(e), is observed. The coercivity of the free layer increases from 87 to 513 Oe on decreasing the temperature from 300 to 50 K; the values increase by about 490% for free layer. The antiferromagnetic coupling field (H_{AFC}) changed from 2062 to 2512 Oe, which represents only 22% increase. We found that the STT switching becomes more symmetric with the temperature drops though the stray field always exists, which provides a potential on canceling the effect of stray field on p-MTJs at low temperature.

IV. CONCLUSION

In conclusion, we have shown the TMR and STT switching behavior of both 84 and 64 nm diameter p-MTJs with double-interface free layer over a wide range of temperature from 400 to 20 K. Our results support the previous reports indicating that the large drop in AP state resistance is induced by thermal magnetic disorder while the P-state conductance is dominated by tunneling electrons. On the contrary, the values of R_P remain almost constant. Low-temperature measurements of magnetic properties suggest that the effect of stray field for STT becomes weaker as the temperature decreases, which provides a hint on the p-MTJs design for cryogenic memories.

ACKNOWLEDGMENT

This work was supported in part by the National Key Technology Program of China under Grant 2017ZX01032101, in part by the National Natural Science Foundation of China under Grant 61571023 and Grant 61627813, in part by the International Collaboration Project under Grant B16001, and in part by the VR innovation platform of Qingdao Science and Technology Commission. Kaihua Cao and Huisong Li contributed equally to this work.

REFERENCES

- [1] H. Yoda *et al.*, “High efficient spin transfer torque writing on perpendicular magnetic tunnel junctions for high density MRAMs,” *Curr. Appl. Phys.*, vol. 10, no. 1, pp. e87–e89, 2010.
- [2] A. D. Kent and D. C. Worledge, “A new spin on magnetic memories,” *Nature Nanotechnol.*, vol. 10, no. 3, pp. 187–191, 2015.
- [3] H.-S. P. Wong and S. Salahuddin, “Memory leads the way to better computing,” *Nature Nanotechnol.*, vol. 10, no. 3, pp. 191–194, Mar. 2015, doi: [10.1038/nnano.2015.29](https://doi.org/10.1038/nnano.2015.29).
- [4] S. H. Kang and C. Park, “MRAM: Enabling a sustainable device for pervasive system architectures and applications,” in *IEDM Tech. Dig.*, Dec. 2017, pp. 38.2.1–38.2.4.
- [5] D. S. Holmes, A. L. Ripple, and M. A. Manheimer, “Energy-efficient superconducting computing—Power budgets and requirements,” *IEEE Trans. Appl. Supercond.*, vol. 23, no. 3, Jun. 2013, Art. no. 1701610.
- [6] D. S. Holmes, A. M. Kadin, and M. W. Johnson, “Superconducting computing in large-scale hybrid systems,” *Computer*, vol. 48, no. 12, pp. 34–42, 2015.
- [7] S. Ikeda *et al.*, “A perpendicular-anisotropy CoFeB–MgO magnetic tunnel junction,” *Nature Mater.*, vol. 9, no. 9, pp. 721–724, Jul. 2010.
- [8] S. Peng *et al.*, “Interfacial perpendicular magnetic anisotropy in sub-20 nm tunnel junctions for large-capacity spin-transfer torque magnetic random-access memory,” *IEEE Magn. Lett.*, vol. 8, pp. 1–5, 2017, Art. no. 3105805. [Online]. Available: <https://ieeexplore.ieee.org/stamp/stamp.jsp?arnumber=7898428>, doi: [10.1109/LMAG.2017.2693961](https://doi.org/10.1109/LMAG.2017.2693961).
- [9] D. C. Worledge, “Theory of spin torque switching current for the double magnetic tunnel junction,” *IEEE Magn. Lett.*, vol. 8, 2017, Art. no. 4306505.
- [10] H. Sato, M. Yamanouchi, S. Ikeda, S. Fukami, F. Matsukura, and H. Ohno, “MgO/CoFeB/Ta/CoFeB/MgO recording structure in magnetic tunnel junctions with perpendicular easy axis,” *IEEE Trans. Magn.*, vol. 49, no. 7, pp. 4437–4440, Jul. 2013.
- [11] H. Sato, M. Yamanouchi, S. Ikeda, S. Fukami, F. Matsukura, and H. Ohno, “Perpendicular-anisotropy CoFeB–MgO magnetic tunnel junctions with a MgO/CoFeB/Ta/CoFeB/MgO recording structure,” *Appl. Phys. Lett.*, vol. 101, no. 2, p. 022414, 2012.
- [12] J. J. Kan, M. Gottwald, C. Park, X. Zhu, and S. H. Kang, “Thermally robust perpendicular STT-MRAM free layer films through capping layer engineering,” *IEEE Trans. Magn.*, vol. 51, no. 12, Dec. 2015, Art. no. 3402105.
- [13] A. A. Timopheev, R. Sousa, M. Chshiev, L. D. Buda-Prejbeanu, and B. Dieny, “Respective influence of in-plane and out-of-plane spin-transfer torques in magnetization switching of perpendicular magnetic tunnel junctions,” *Phys. Rev. B, Condens. Matter*, vol. 92, no. 10, p. 104430, 2015.
- [14] M. Wang *et al.*, “Current-induced magnetization switching in atom-thick tungsten engineered perpendicular magnetic tunnel junctions with large tunnel magnetoresistance,” *Nature Commun.*, vol. 9, Feb. 2018, Art. no. 671.
- [15] C. H. Shang, J. Nowak, R. Jansen, and J. S. Moodera, “Temperature dependence of magnetoresistance and surface magnetization in ferromagnetic tunnel junctions,” *Phys. Rev. B, Condens. Matter*, vol. 58, no. 6, pp. R2917–R2920, 1998.
- [16] A. A. Khan *et al.*, “Elastic and inelastic conductance in Co-Fe-B/MgO/Co-Fe-B magnetic tunnel junctions,” *Phys. Rev. B, Condens. Matter*, vol. 82, no. 6, p. 064416, 2010.
- [17] Y. Takeuchi, H. Sato, S. Fukami, F. Matsukura, and H. Ohno, “Temperature dependence of energy barrier in CoFeB–MgO magnetic tunnel junctions with perpendicular easy axis,” *Appl. Phys. Lett.*, vol. 107, no. 15, p. 152405, 2015.
- [18] L. Yuan, S. H. Liou, and D. Wang, “Temperature dependence of magnetoresistance in magnetic tunnel junctions with different free layer structures,” *Phys. Rev. B, Condens. Matter*, vol. 73, no. 13, p. 134403, 2006.
- [19] V. Drewello, J. Schmalhorst, A. Thomas, and G. Reiss, “Evidence for strong magnon contribution to the TMR temperature dependence in MgO based tunnel junctions,” *Phys. Rev. B, Condens. Matter*, vol. 77, no. 1, p. 014440, 2008.
- [20] J. J. Kan, K. Lee, M. Gottwald, S. H. Kang, and E. E. Fullerton, “Low-temperature magnetic characterization of optimum and etch-damaged in-plane magnetic tunnel junctions,” *J. Appl. Phys.*, vol. 114, p. 114506, Aug. 2013.
- [21] T. Newhouse-Illige *et al.*, “Temperature dependence of interlayer coupling in perpendicular magnetic tunnel junctions with GdO_x barriers,” *Appl. Phys. Lett.*, vol. 112, no. 7, p. 072404, 2018.
- [22] W. Skowroński *et al.*, “Understanding stability diagram of perpendicular magnetic tunnel junctions,” *Sci. Rep.*, vol. 7, Aug. 2017, Art. no. 10172.
- [23] S. Bandiera *et al.*, “Comparison of synthetic antiferromagnets and hard ferromagnets as reference layer in magnetic tunnel junctions with perpendicular magnetic anisotropy,” *IEEE Magn. Lett.*, vol. 1, pp. 1–4, 2010, Art. no. 3000204. [Online]. Available: <https://ieeexplore.ieee.org/stamp/stamp.jsp?tp=&arnumber=5504576>, doi: [10.1109/LMAG.2010.2052238](https://doi.org/10.1109/LMAG.2010.2052238).
- [24] Y. Wang, H. Cai, L. A. B. Naviner, Y. Zhang, J. O. Klein, and W. S. Zhao, “Compact thermal modeling of spin transfer torque magnetic tunnel junction,” *Microelectron. Reliab.*, vol. 55, nos. 9–10 pp. 1649–1653, 2015.
- [25] X.-F. Han, A. C. C. Yu, M. Oogane, J. Murai, T. Daibou, and T. Miyazaki, “Analyses of intrinsic magnetoelectric properties in spin-valve-type tunnel junctions with high magnetoresistance and low resistance,” *Phys. Rev. B, Condens. Matter*, vol. 63, no. 22, p. 224404, 2001.
- [26] S. Yuasa, T. Nagahama, A. Fukushima, Y. Suzuki, and K. Ando, “Giant room-temperature magnetoresistance in single-crystal Fe/MgO/Fe magnetic tunnel junctions,” *Nature Mater.*, vol. 3, pp. 868–871, Oct. 2004.
- [27] Y. Zhang *et al.*, “Compact modeling of perpendicular-anisotropy CoFeB/MgO magnetic tunnel junctions,” *IEEE Trans. Electron Devices*, vol. 59, no. 3, pp. 819–826, Mar. 2012.
- [28] L. Thomas *et al.*, “Probing magnetic properties of STT-MRAM devices down to sub-20 nm using spin-torque FMR,” in *IEDM Tech. Dig.*, pp. 38.4.1–38.4.4, Dec. 2017.
- [29] Y. H. Wang *et al.*, “Impact of stray field on the switching properties of perpendicular MTJ for scaled MRAM,” in *IEDM Tech. Dig.*, pp. 29.2.1–29.2.4, Dec. 2012.
- [30] R. Matsumoto *et al.*, “Spin-torque-induced switching and precession in fully epitaxial Fe/MgO/Fe magnetic tunnel junctions,” *Phys. Rev. B, Condens. Matter*, vol. 80, no. 17, p. 174405, 2009.
- [31] J. G. Alzate *et al.*, “Temperature dependence of the voltage-controlled perpendicular anisotropy in nanoscale MgO|CoFeB|Ta magnetic tunnel junctions,” *Appl. Phys. Lett.*, vol. 104, p. 112410, Mar. 2014.